Journal of Alloys and Compounds 509 (2011) 1819–1823

Contents lists available at ScienceDirect

Journal of Alloys and Compounds

journal homepage: www.elsevier.com/locate/jallcom

Synthesis, microstructure and mechanical properties of reaction-infiltrated TiB_2–SiC–Si composites

WuBian Tian*, Hideki Kita, Hideki Hyuga, Naoki Kondo

National Institute of Advanced Industrial Science and Technology (AIST), 2266-98 Anagahora, Shimo-Shidami, Moriyama-ku, Nagoya 463-8560, Japan

ARTICLE INFO

Article history:
Received 5 August 2010
Received in revised form 8 October 2010
Accepted 10 October 2010
Available online 21 October 2010

Keywords:
TiB_2–SiC–Si composite
Reactive melt infiltration
Microstructure
Mechanical properties

ABSTRACT

TiB_2–C preforms formed with different compositions and processing parameters were reactively infiltrated by Si melts at 1450 °C to fabricate TiB_2–SiC–Si composites. Phase constituent and microstructure of these composites were analyzed by X-ray diffraction (XRD) and scanning electron microscopy (SEM). The resulting composites are generally composed of TiB_2 and reaction-formed β-SiC major phases, together with a quantity of residual Si. Unreacted carbon is detected in the samples with a starting composition of $2TiB_2 + 1C$ formed at higher pressure and in all of the ones at the composition of $1TiB_2 + 1C$. The distribution of these phases is fairly homogeneous in microstructure. TiB_2–SiC–Si composites show good mechanical properties, with representative values of 19.9 GPa in hardness, 395 GPa in elastic modulus, 3.5 MPa $m^{1/2}$ in fracture toughness and 604 MPa in bending strength. The primary toughening and strengthening mechanism is attributed to the crack deflection of TiB_2 particles.

1. Introduction

Reaction-bonded silicon carbide (RBSC) was firstly introduced by Popper in 1960s [1,2] and subsequently developed by other investigators [3–5]. This technique contains the reactive infiltration of silicon melt into a preform typically containing SiC and carbon powders combined with polymer binders. The resultant materials consist of the original SiC, reaction-formed SiC and residual Si. The merits of RBSC processes are the low processing temperature and the near net-shape ability as compare it with conventional ceramics processing methods [6]. In addition, RBSC was reported to exhibit good mechanical properties at room temperature while the highest service temperature was limited to the melting point of silicon (~1410 °C) [7,8].

Variants of RBSC were made by Hucke et al. [9,10] and Chiang et al. [6,11], in which a polymer-derived carbon preform was used to fabricate dense SiC–Si composites. Furthermore, RBSC was modified by replacing original SiC with B_4C [12,13] or incorporating other carbides as additives together with TiB_2 as the microcrack toughening phase [14]. Here, we present a modified reaction bonding process to prepare TiB_2–SiC–Si composite through the infiltration of Si melt to TiB_2–C preform. The processing, microstructure and mechanical properties of this novel material are evaluated and discussed.

2. Experimental procedure

Titanium boride (1.65 μm, Grade NF) and pure carbon (5 μm, purity of 99.7%) with addition of 1 wt.% dispersant and 3 wt.% binder were ball milled for 24 h in ethanol. The weight ratio of TiB_2 to carbon was selected to be 2:1 or 1:1. The free carbon come from the dispersant and binder is less than 0.3 wt.% and therefore is not to be concerned. The mixtures were dried with a rotary evaporator, crushed and screened through a 150 mesh sieve. Green compacts, ~Φ20 mm × 5 mm, were formed by uniaxial pressing at about 20 MPa, followed by CIPing at 200 MPa or 400 MPa. Then the compacts were debinded at 600 °C in N_2 or at 1500 °C in vacuum for 2 h to pyrolyze binder. Finally, the porous TiB_2–C preforms were infiltrated with silicon melt at 1450 °C for 1 h in vacuum. The heating rate was 10 °C/min, and the cooling rate was 10 °C/min from 1450 °C to 1200 °C, followed by furnace cooling. These testing conditions were summarized in Table 1, including the sample label and the measured properties of infiltrated composites. The sample label obeyed the following rules: 1) the first number and the following two letters reminded the weight ratio of TiB_2 to carbon; 2) the numbers after dash suggested the CIP forming pressure and the debinding temperature. For example, 2TC-215 meant that the preform was composed of TiB_2 and carbon with a weight ratio of 2:1, CIPed under 200 MPa, debinded at 1500 °C and finally infiltrated in vacuum.

The green densities of preforms were calculated from the measured weights and dimensions. Bulk densities of infiltrated samples were measured by the Archimedes method. Phase constituents were determined by X-ray diffractometry (XRD, RINT2000, Rigaku, Japan) with Cu K_α radiation on the ground surface of sample. The residual Si fraction in the composite was calculated from the measured bulk density (d_m) and the theoretical densities of Si, SiC and TiB_2 (here, $d_{Si} = 2.33$ g/cm^3, $d_{SiC} = 3.21$ g/cm^3 and $d_{TiB_2} = 4.56$ g/cm^3), according to the following equations.

$$V_{Si} + V_{SiC} + V_{TiB_2} = 1 \quad (1)$$

$$d_{Si} \times V_{Si} + d_{SiC} \times V_{SiC} + d_{TiB_2} \times V_{TiB_2} = d_m \quad (2)$$

$$d_{TiB_2} \times \frac{V_{TiB_2}}{d_{SiC} \times V_{SiC}} = n \times \frac{MW_C}{MW_{SiC}} \quad (3)$$

* Corresponding author. Tel.: +81 52 736 7120; fax: +81 52 736 7405.
E-mail address: w.b.tian@aist.go.jp (W. Tian).

0925-8388/$ – see front matter © 2010 Elsevier B.V. All rights reserved.
doi:10.1016/j.jallcom.2010.10.053

$$V_{Si} = \frac{(d_{TiB_2} \times (d_{SiC} + d_{SiC} \times n \times MW_C/MW_{SiC})) - (d_m \times (d_{TiB_2} + d_{SiC} \times n \times MW_C/MW_{SiC}))}{(d_{TiB_2} \times (d_{SiC} + d_{SiC} \times n \times MW_C/MW_{SiC})) - (d_{Si} \times (d_{TiB_2} + d_{SiC} \times n \times MW_C/MW_{SiC}))} \quad (4)$$

where V_{Si}, V_{SiC} and V_{TiB_2} were the volume fraction of Si, SiC and TiB_2 respectively, n was the weight ratio of TiB_2 to carbon, MW_C and MW_{SiC} were the molecular weight of carbon and SiC respectively. Note that this calculation was not suitable for the composite containing unreacted carbon.

Microstructure observations on the polished surface and the fracture surface were performed via scanning electron microscope (JSM-5600, JEOL, Japan) equipped with energy dispersive spectrometer (EDS JED-2300, JEOL, Japan). Vickers hardness was determined by means of indentation method (MVK-G3 hardness tester, Akashi, Japan) with a load of 19.6 N for 15 s. Ten indentations were made on the polished surface for each sample. Fracture toughness was evaluated by measuring the crack length after Vickers hardness tests and calculated using the following equation proposed by Anstis et al. [15].

$$k_{IC} = 0.016 \times \left(\frac{E}{H_V}\right)^{0.5} \times \left(\frac{P}{c_0^{1.5}}\right) \quad (5)$$

where E is the Young's modulus, H_V is the Vickers hardness, P is the indentation load and c_0 is the square root of the measured crack lengths c_1 and c_2. Young's modulus was measured by the pulse-echo method and was the average of three measurements. A green compact with a dimension of 45 mm × 45 mm × 5 mm was used for the infiltration test and the strength measurement. 4-point bending strength was measured on 4 mm × 3 mm × 40 mm beams with outer and inner span of 30 mm and 10 mm, respectively, at a crosshead speed of 0.5 mm/min. The tensile surfaces of the specimens were polished to a 0.5 μm diamond finish and the edges of tested specimens were beveled. At least 5 bars were used for the strength measurements.

3. Results and discussion

3.1. XRD analysis

At a fixed TiB_2/C ratio of 2, i.e., 2TC series, the XRD patterns of the TiB_2–SiC–Si composites infiltrated at 1450 °C for 1 h are shown in Fig. 1. It is clear that the prepared samples are composed of TiB_2 and reaction-formed β-SiC major phases, together with a quantity of residual Si. Unreacted carbon is detected in the samples CIPed at higher pressure. The forming pressure and debinding temperature are found to influence the phase constituents of resultant composites, mainly the residual Si fraction. Because all of the XRD patterns in Fig. 1 are conducted in the fairly identical testing conditions and have been normalized, it is reasonable to semi-quantitatively evaluate the residual Si fraction with the integrated intensity of Si peak at 28.4°.

Under the same forming pressure, the composite debinded at higher temperature contains more residual Si. For example, the residual Si fraction of sample 2TC-215 preheated at 1500 °C (21 vol.%) is higher than that of sample 2TC-206 debinded at 600 °C (19 vol.%), presuming the complete transformation of carbon in starting powder into SiC. This is because the high debinding temperature leads to a fast debinding rate and thus a strong mass loss of preform within the same time, including the binder and possibly the impurities of starting TiB_2 and carbon, which results in high porosity and subsequently a large amount of residual Si. In addition, after debinded at the same temperature, the preform CIPed at higher pressure results in the composite containing lessresidual Si and a small amount of carbon, which is attributed to the increased green density of preform (Table 1) that leads to the lower porosity and the more difficult penetration of Si melt.

For the $1TiB_2 + 1C$ preforms (1TC series), the effect of forming pressure and debinding temperature on the phase constituents of TiB_2–SiC–Si composites is also investigated and the corresponding XRD results are shown in Fig. 2. The resulting composites consist of TiB_2, reaction-formed SiC, residual Si and unreacted carbon, in which SiC instead of TiB_2 displays the strongest peak. The residual Si fraction is found to increase with debinding temperature but decrease with forming pressure as keeping the other processing parameters the same, which is similar to that of 2TC samples, as discussed above. The amount of unreacted carbon in 1TC samples is higher than that of 2TC ones when fabricated at the same conditions, demonstrating that the accomplishment of reactive infiltration becomes difficult with the increase of carbon content in preforms, which is more evident in the samples formed at higher pressure.

3.2. SEM examination

Backscattered SEM micrographs of the infiltrated 2TC samples are shown in Fig. 3(a) through (d). The XRD results suggest that these samples predominantly consist of TiB_2, SiC and Si phases and small amount of carbon is detected in sample 2TC-406 and 2TC-415

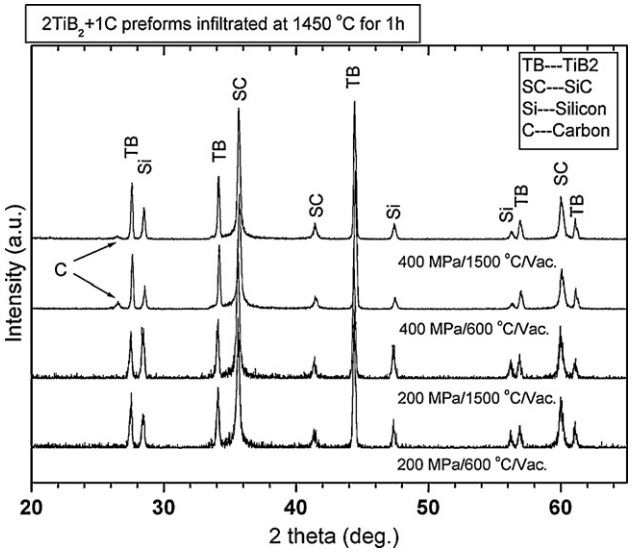

Fig. 1. The XRD patterns of $2TiB_2 + 1C$ preforms prepared at different conditions and infiltrated at 1450 °C for 1 h.

Table 1
Summary of the starting composition, processing parameters, measured density and mechanical properties of TiB_2–SiC–Si composites reaction-infiltrated at 1450 °C for 1 h (W_r: weight ratio of TiB_2 to carbon, P_f: CIP forming pressure, T_d: debinding temperature, d_g: calculated green density of preform after CIP forming and debinding, d_m: measured density, R_{Si}: residual Si fraction, H_V: Vickers hardness, E: elastic modulus, K_{IC}: fracture toughness).

Sample label	W_r TiB_2:C	P_f (MPa)	T_d (°C)	d_g (g/cm^3)	d_m (g/cm^3)	R_{Si} (vol. %)	H_V (GPa)	E (GPa)	K_{IC} (MPa m$^{1/2}$)
2TC-206	2:1	200	600	1.86	3.37	18.6	20.6 ± 1.1	397 ± 1	3.6 ± 0.4
2TC-215	2:1	200	1500	1.75	3.34	21.4	19.9 ± 1.3	395 ± 5	3.5 ± 0.4
2TC-406	2:1	400	600	2.02	3.45	–	22.4 ± 0.6	397 ± 2	3.9 ± 0.2
2TC-415	2:1	400	1500	1.91	3.41	–	21.1 ± 0.9	410 ± 3	3.5 ± 0.3
1TC-206	1:1	200	600	2.10	3.32	–	21.9 ± 1.0	380 ± 5	3.2 ± 0.3
1TC-215	1:1	200	1500	1.93	3.27	–	21.5 ± 0.6	363 ± 9	2.9 ± 0.2
1TC-406	1:1	400	600	2.21	3.28	–	21.1 ± 1.0	323 ± 19	2.6 ± 0.1
1TC-415	1:1	400	1500	2.08	3.27	–	20.1 ± 1.0	320 ± 5	3.5 ± 0.4

–, residual Si fraction cannot be calculated because of the presence of unreacted carbon.

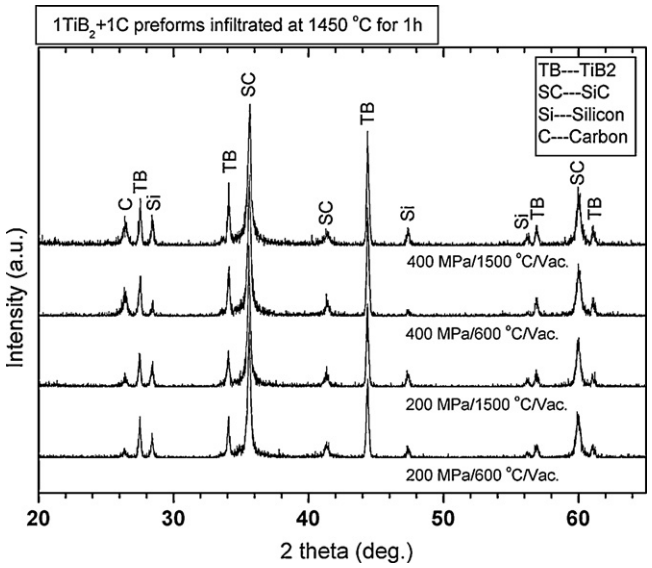

Fig. 2. The XRD patterns of $1TiB_2 + 1C$ preforms prepared at different conditions and infiltrated at 1450 °C for 1 h.

(see Fig. 1). The SEM images agree well with the XRD results. For instance, in composite 2TC-206 and 2TC-215, the obtained samples show homogeneous microstructure, in which the bright TiB_2 particles distribute homogeneously in gray mixed phases of SiC and Si. And in the case of sample 2TC-406 and 2TC-415, some dark phases found to be rich in element C by the EDS analysis (not shown) are coincident with the unreacted carbon. It should be noted that the color contrast between SiC and Si is not distinct here due to the complicated phase constituents. The estimation of residual Si from microstructure, therefore, is not conducted in present work.

For the 1TC samples, all of the infiltrated composites contain the dark carbon phase and its content rises remarkably with the increase of forming pressure, which can be clearly seen from the microstructures in Fig. 4(a)–(d). Note that the microstructure of 1TC composites is fairly homogeneous. In addition, the volume fraction of TiB_2 phase decreases due to the declining TiB_2/C ratio in starting composition. Although most of the composites are nearly full dense on the basis of the microstructure observations, a quantity of dark pores are found in the sample 2TC-406 and 1TC-406 (indicated by arrows in Figs. 3(c) and 4(c)), suggesting that the forming pressure and debinding temperature affect not only the phase constituents but also the densification of microstructure in TiB_2–SiC–Si composites.

3.3. Mechanical properties

The mechanical properties of fabricated TiB_2–SiC–Si composites, such as hardness, elastic modulus and fracture toughness, are summarized in Table 1. The measured properties are found to correlate with the phase constituents, density and microstructure. For example, the phase constituents of prepared composites consist of relatively hard phases such as TiB_2 and SiC and soft phases like Si and carbon. For the same starting preforms, the resulted samples containing higher fraction of Si and/or carbon show lower hardness. With a close fraction of soft phases, 1TC samples usually exhibit higher hardness than 2TC ones because of the larger amount of hard SiC phase. Elastic modulus is found to be predominantly affected by the phase content and related to the porosity of sample. The lower modulus of 1TC relative to 2TC is mainly attributed to the less amount of stiff TiB_2 phase and the larger amount of soft carbon phase. The fracture toughness is closely correlated with the TiB_2 content because the toughening mechanism in these systems is the cracking deflection effect of TiB_2 particles, as discussed below,

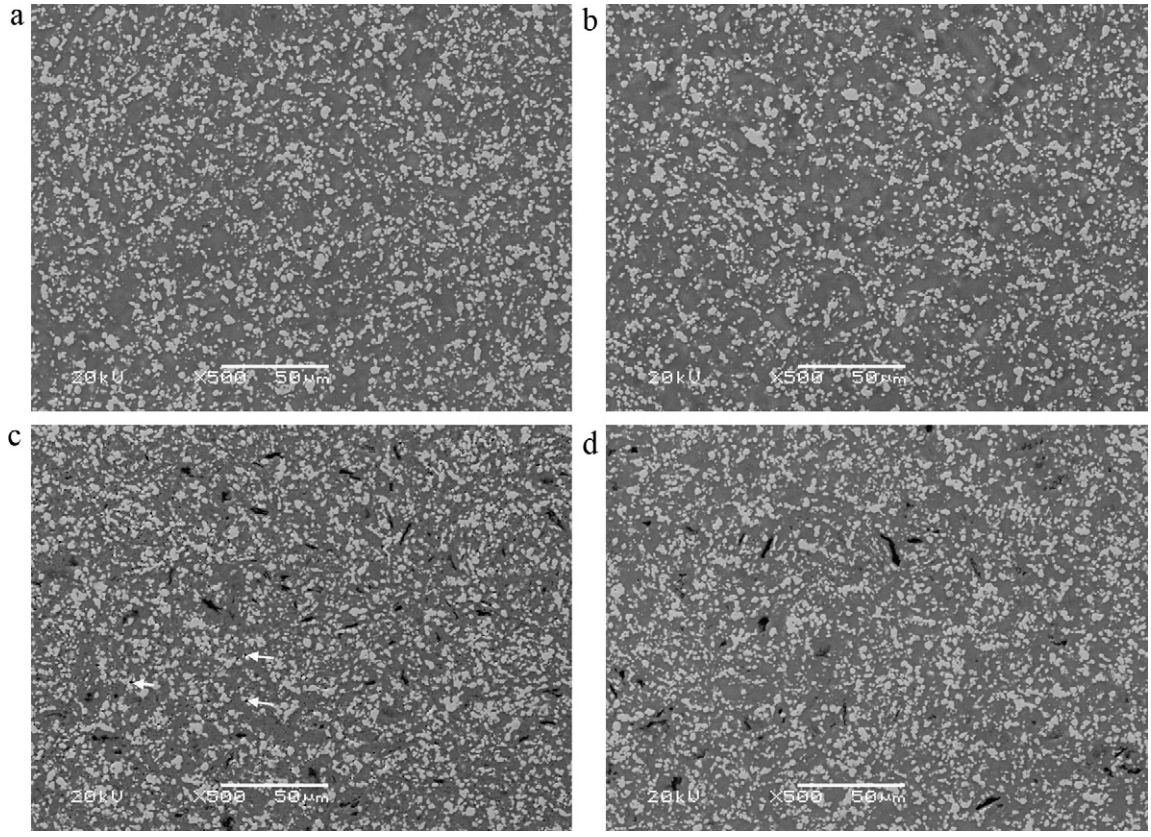

Fig. 3. Backscattered SEM micrographs of the infiltrated (a) 2TC-206, (b) 2TC-215, (c) 2TC-406 and (d) 2TC-415 samples.

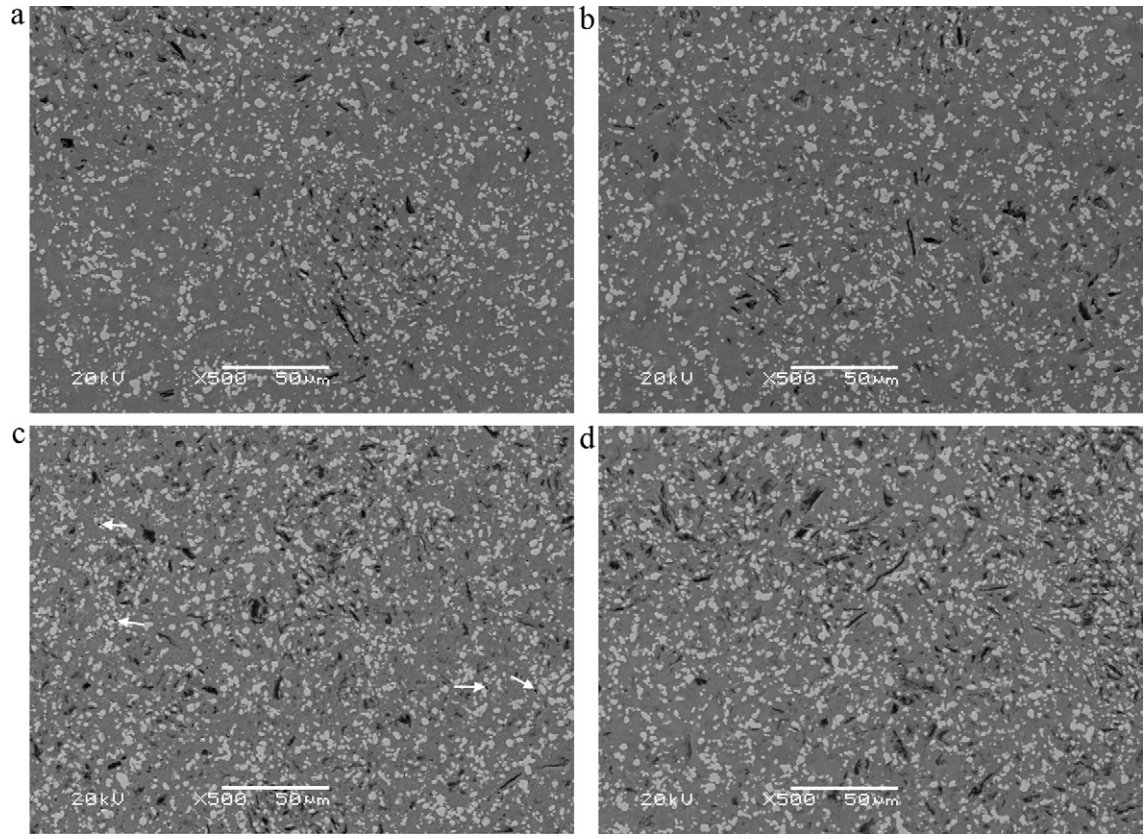

Fig. 4. Backscattered SEM examinations on the polished surfaces of infiltrated (a) 1TC-206, (b) 1TC-215, (c) 1TC-406 and (d) 1TC-415 composites.

which is confirmed by the relatively lower fracture toughness of 1TC samples that containing less amount of TiB_2 phase.

Here, we make a detailed annotation to the well infiltrated composite 2TC-215 for clarity and compared with the broadly studied reaction-bonded SiC [5,11,12] and B_4C [12,13]. The hardness of composite TiB_2–SiC–Si is around 19.9 GPa, which is usually close to those of RBSC (17–22 GPa) and generally smaller than those of composites B_4C–SiC–Si (20–28 GPa). This is attributed to the different phase hardness and residual Si fraction in composites. The fracture toughness of composite 2TC-215 is 3.5 MPa $m^{1/2}$, which is comparable to the RBSC (3.5–4.5 MPa $m^{1/2}$) but lower than B_4C–SiC–Si composites (5.0–7.9 MPa $m^{1/2}$). A typical crack propagation path of sample 2TC-215 is shown in Fig. 5(a), in which the crack propagates straightly in both Si and SiC areas but changes its direction by the deflection of TiB_2 particles (indicated by white arrows). The thermal mismatch between TiB_2 and SiC/Si and the weak interface around TiB_2 particles are responsible for this phenomenon. Crack deflection was also found in the in situ synthesized TiB_2 toughened SiC [16], which contributed to the fracture toughness. With a value of 395 GPa, the elastic modulus of composite 2TC-215 is comparable to those of composites SiC–Si and B_4C–SiC–Si. Considering the high theoretically elastic modulus of TiB_2 [17], the modulus of composite TiB_2C–SiC–Si is expected to be tailored by adjusting the TiB_2 content in obtained samples.

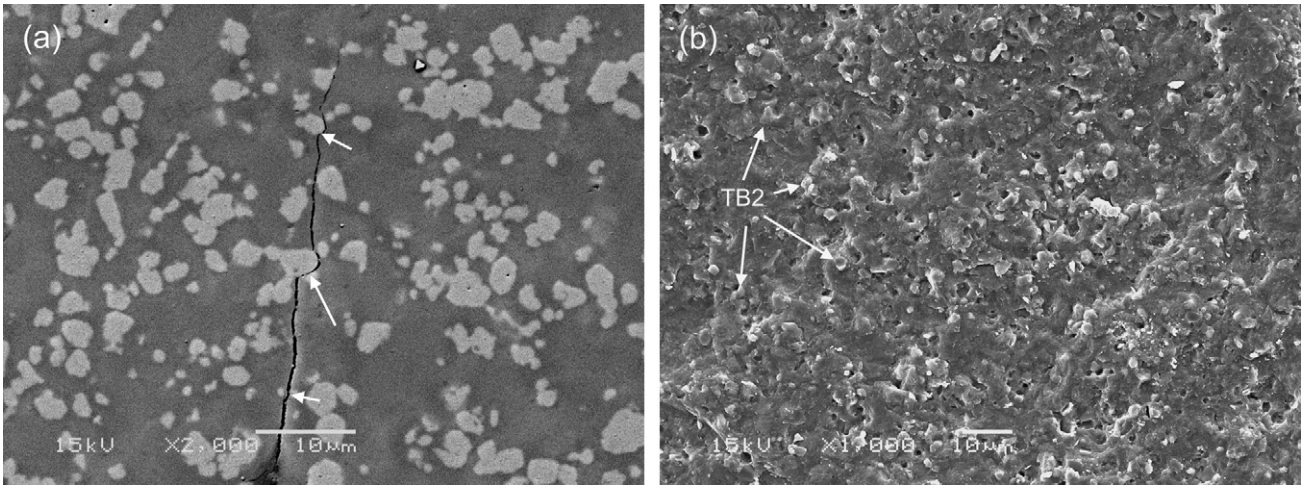

Fig. 5. (a) Typical crack propagation path of sample 2TC-215. The white arrows denote the deflection of TiB_2 particle to crack. (b) Representative fracture surface of TiB_2–SiC–Si composite. The hindering and deflecting effects of TiB_2 particles on fracture are denoted by white arrows.

Furthermore, the bending strength of composite 2TC-215 is measured to be 604 MPa, which is higher or at least comparable with the reaction-bonded composites [5,11–13]. This is an indication of good strengthening effect of TiB_2 phase. A representative fracture surface of TiB_2–SiC–Si composite is given in Fig. 5(b), from which the hindering and deflecting effects of TiB_2 particles (denoted by white arrows) on fracture are evident. As the cracking propagates from the left to the right, the fracture surface forwards not flat but wavily due to the presence of TiB_2 particles. The relatively rough surface implies more fracture surface energy required and thus higher mechanical strength achieved. Note that the hardness, elastic modulus and mechanical strength of this composite could be improved if reducing the relatively high fraction of residual Si.

4. Conclusions

TiB_2–C preforms, prepared with different TiB_2/C ratios, forming pressure and debinding temperature, were reactively infiltrated by Si melts at 1450 °C to synthesize TiB_2–SiC–Si composites. The resulting composites generally consist of TiB_2 and reaction-formed β-SiC major phases, together with a quantity of residual Si. Unreacted carbon is detected in the 2TC samples formed at higher pressure and in all of the 1TC ones. The residual Si fraction is found to increase with debinding temperature but decrease with forming pressure and the amount of unreacted carbon in 1TC samples is usually higher than that of 2TC ones. The distribution of these phases is fairly homogeneous in microstructure. The mechanical properties of TiB_2–SiC–Si composites, with representative values of 19.9 GPa in hardness, 395 GPa in elastic modulus, 3.5 MPa $m^{1/2}$ in fracture toughness and 604 MPa in bending strength, are found to correlate with the phase constituents, density and microstructure. Furthermore, the crack deflection of TiB_2 particles is found to be the primary toughening and strengthening mechanism.

Acknowledgements

The present research was carried out with financial aid from New Energy and Industrial Technology Development Organization (NEDO) as part of the "Innovative Development of Ceramics Production Technology for Energy Saving". The authors would like to appreciate NEDO and all the other related parties for their support.

References

[1] P.P. Popper, Special Ceramics, Heywood, London, 1960.
[2] P.P. Popper, Production of dense bodies of silicon carbide, U.S. Patent 3275722, February 17, 1966.
[3] K.M. Taylor, Cold molded dense silicon carbide articles and methods of making the same, U.S. Patent 3205043, September 7, 1965.
[4] C.W. Forrest, P. Kennedy, J.V. Shennan, Special Ceramics, British Ceramic Research Association, Stoke-on-Trent, 1972.
[5] S. Suyama, T. Kameda, Y. Itoh, Diamond Relat. Mater. 12 (2003) 1201–1204.
[6] Y.M. Chiang, R.P. Messner, C.D. Terwilliger, D.R. Behrendt, Mater. Sci. Eng. A 144 (1991) 63–74.
[7] O. Chakrabarti, S. Ghosh, J. Mukerji, Ceram. Int. 20 (1994) 283–286.
[8] J.M. Fernández, A. Muñoz, A.R.D. Arellano López, F.M.V. Feria, A. Dominguez-Rodriguez, M. Singh, Acta Mater. 51 (2003) 3259–3275.
[9] E.E. Hucke, Composite bodies comprising a continuous framework and an impregnated metallic material and methods of their production, U.S. Patent 3235346, February 15, 1966.
[10] E.E. Hucke, Process development for silicon carbide based structural ceramics, AMMRC Tech. Rep. TR 83-5, US Army Materials and Mechanics Research Center, January 1983.
[11] L. Hozer, J.R. Lee, Y.M. Chiang, Mater. Sci. Eng. A 195 (1995) 131–143.
[12] M.K. Aghajanian, B.N. Morgan, J.R. Singh, J. Mears, R.A. Wolffe, Ceram. Trans. (USA) 134 (2001) 527–539.
[13] S. Hayun, D. Rittel, N. Frage, M.P. Dariel, Mater. Sci. Eng. A 487 (2008) 405–409.
[14] A.J. Whitehead, T.F. Page, J. Mater. Sci. 27 (1992) 839–852.
[15] G.R. Anstis, P. Chantikul, B.R. Lawn, D.B. Marshall, J. Am. Ceram. Soc. 64 (1981) 533–538.
[16] G.J. Zhang, X.M. Yue, Z.Z. Jin, J.Y. Dai, J. Eur. Ceram. Soc. 16 (1996) 409–412.
[17] R.G. Munro, J. Res. Natl. Inst. Stand. Technol. 105 (2000) 709–720.